

ANALYSIS OF FRICTION CHARACTERISTIC PARAMETERS IMPACT ON VIBRATION OF COUPLE OF BLADES WITH FRICTION ELEMENT

Jan Brůha*, Vladimír Zeman*

Presented work concerns with a sensitivity analysis of a harmonically excited bending vibration of a rotating couple of blades with a friction element with regard to the parameters of the friction characteristic. Either of the blades is discretized by FEM using beam elements and continuously distributed weight is concentrated in nodal points. The friction in central contact points between blade shrouds and the friction element is approximated by a continuous function depending on slip velocities of the shrouds relative to the friction element. Considered friction characteristic respects the micro-slip phase at the very low slip velocities and the macro-slip (full-slip) phase at the higher slip velocities. The values of the friction characteristic parameters are identified by comparison of the numerical simulations of a transient vibration with experiments used in IT AS CR.

Keywords: blade vibration, dry friction, friction characteristic parameters, sensitivity analysis, numerical simulation

1. Introduction

While power plants are still projected more powerful and effective, demands on reliability of these machines are rising. Blade vibrations as a side effect the operation of steam turbines are very dangerous because of the high cycle fatigue failure. One of the basic methods of bladed disk vibrations suppression is inserting friction elements between blade shrouds. Dissipation of energy, due to dry friction between the blade shroud surfaces and the friction element surfaces, or using detuning masses mounting on certain blade shrouds belong to basic methods of bladed disk vibrations suppression. Detail investigation of influences of a friction (mainly the friction phenomenon) on a dynamical response of a beam can be found in [1]. Some publications deal with the friction induced by means of friction elements inserted between the blades. A method for the calculation of a static balance supposing an in-plane motion of the wedge friction element is discussed in [2]. An analytical approach is described in [3] and comparison of numerical simulation results with the results obtained by linearization is shown in [4]. The equivalent linearization method for the evaluation of friction effects can be used as the first approximation by means of so-called equivalent viscous damping [5]. This method has been experimentally verified in [6] and applied in the Department of Mechanics of University of West Bohemia in Pilsen to the harmonic forced vibration of two rotating blades with friction damping [7]. The friction impact in contact areas between the blade shrouds and the friction element embedded between the shrouds on

* Bc. J. Brůha, prof. Ing. V. Zeman, DrSc., Department of Mechanics, Faculty of Applied Sciences, University of West Bohemia in Pilsen, Univerzitní 22, 306 14 Plzeň

blade vibrations has been experimentally researched in a frame of the grant project GA CR 101/09/1166 ‘Research of dynamic behavior and optimization of complex rotating system with non-linear couplings and high damping materials’ in the Institute of Thermomechanics of the Academy of Sciences of the Czech Republic (IT AS CR) [8], [9]. In accordance with the experimental arrangement tested in IT AS CR (Figure 1), the computational model of a couple of clamped blades into a horizontal situated non-rotating ($\omega_0 = 0$) rigid disk (Figure 2) has been designed.

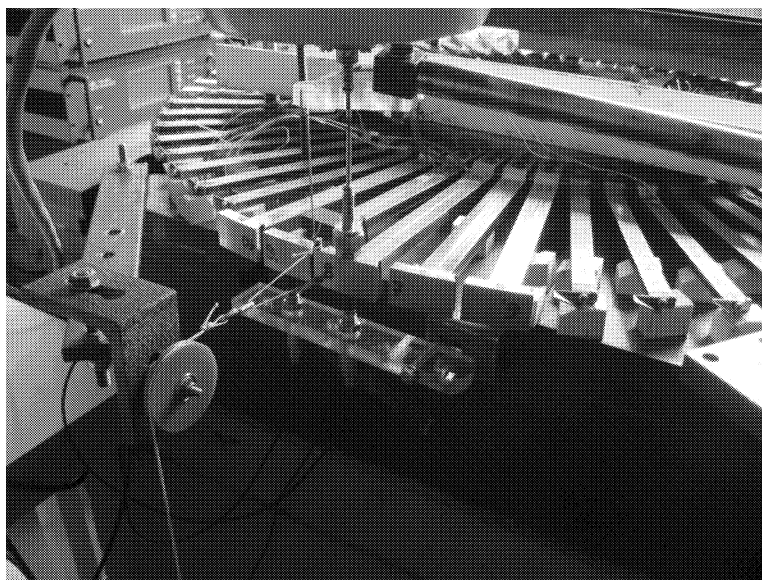


Fig.1: Experimental arrangement tested in IT AS CR

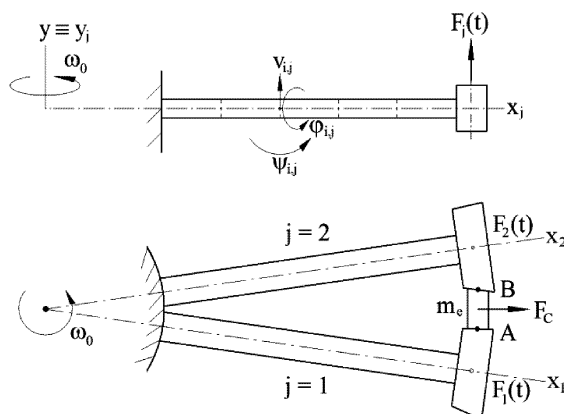


Fig.2: Physical model of the couple of blades with friction element

In the article [10], it has been investigated a detuning of blades caused by an additional mass mounted on one of the blade shroud and friction impact on harmonically excited bending vibration suppression. The characteristics of frictional forces in contact areas have been approximated by the continuous function \tanh with the argument expressed slip velocity

of the central contact point of the blade shroud relative to the friction element multiplied by a constant defining an inclination of this function for very low slip velocity. Experimentally ascertained results with an ARAMID friction element [11] as well as computational analysis of various types of dry friction characteristics [12] have proved significant micro- and macro-slip phases impact. However, assuming the friction characteristic is approximated by tgh function, separation of these phases is very difficult. Therefore, the aim of this article is to analyze chosen parameters impact of more sophisticated characteristic of frictional forces [13] on transversely excited vibration of couple of blades clamped into a rigid rotating disk with a friction element placed between blade shrouds. For the reason that we also want to analyze rotating impact on the blade vibrations, the mathematical model of the couple of blades with the friction element is generalized and respects inertial effects under rotation with constant angular velocity.

2. Mathematical model of a blade in rotating space

To discretize the blade in rotating space, it has been necessary to derive one-dimensional beam element's matrices in local coordinate system of the blade rotating with angular velocity ω_0 . We assume a bending vibration of the blade in its plane of symmetry \widehat{xy} combined with a torsional vibration along the longitudinal axis. The spatial motion of a blade's mass element with length dx and at distance x to the origin of the beam element between nodes $i - 1$ and i can be described by translational motion with the velocity of the mass centre s expressed in coordinate system xyz (Figure 3) by vector

$$\mathbf{v}_s(x, t) = [0, \dot{v}(x, t), -\omega_0(r_{i-1} + x)]^T, \tag{1}$$

where r_{i-1} is perpendicular distance (radius) of the initial blade's element node $i - 1$ from axis of rotation y (see Figure 3), and relative spherical motion around this centre. The immediate angular velocity is described by vector

$$\boldsymbol{\omega} = [\dot{\varphi}(x, t) + \omega_0 \sin \psi(x, t), \omega_0 \cos \psi(x, t), \dot{\psi}(x, t)]^T \tag{2}$$

expressed in coordinate system $\xi\eta\zeta$, where $\widehat{\eta\zeta}$ is the plane of the blade's cross-section after deformation. As a consequence, deformations in place x of the blade's element are described by transversal displacement $v(x, t)$, flexural displacement $\psi(x, t)$ and torsional displacement $\varphi(x, t)$ of the cross-section.

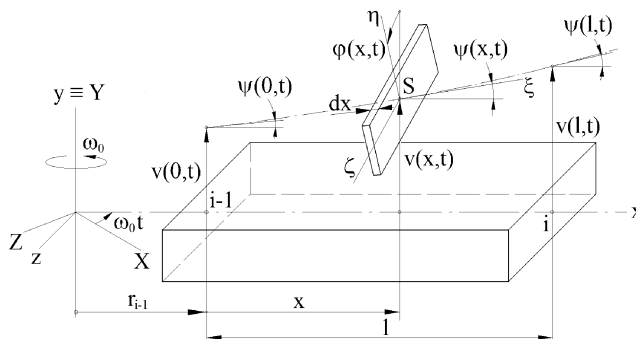


Fig.3: Deformation of the blade's element

Let us suppose, the flexural $\psi(x, t)$ and torsional $\psi(x, t)$ displacements are small. Then, the mathematical model of the undamped beam element of the blade between the nodes $i - 1$ and i can be derived in configuration space

$$\mathbf{q}^{(e)} = [v_{i-1}, \psi_{i-1}, v_i, \psi_i, \varphi_{i-1}, \varphi_i]^T, \quad (3)$$

where $v_{i-1} = v(0, t)$, $\psi_{i-1} = \psi(0, t)$, $v_i = v(l, t)$, $\psi_i = \psi(l, t)$, $\varphi_{i-1} = \varphi(0, t)$, $\varphi_i = \varphi(l, t)$. The kinetic energy of the finite blade's element with length l , cross-section area A and material density ρ can be expressed in the form

$$E_k^{(e)} = \frac{1}{2} \int_0^l [A \mathbf{v}_s^T(x, t) \mathbf{v}_s(x, t) + \boldsymbol{\omega}^T(x, t) \mathbf{J} \boldsymbol{\omega}(x, t)] \rho dx, \quad (4)$$

where the inertia matrix of the blade's mass element $\mathbf{J} \rho dx$ is described by matrix of the second moments of area of cross-section

$$\mathbf{J} = \begin{bmatrix} J_\eta + J_\zeta & 0 & 0 \\ 0 & J_\eta & 0 \\ 0 & 0 & J_\zeta \end{bmatrix} \quad (5)$$

about the major axes of cross-section $\eta\zeta$. The potential energy of deformation of the blade's element is expressed as [14]

$$E_p^{(e)} = \frac{1}{2} \int_0^l \int_{(A)} \{ E \varepsilon_x^2(x, t) + G [\gamma_{xy}^2(x, t) + \gamma_{xz}^2(x, t)] \} dA dx, \quad (6)$$

where E is Young's modulus and G is shear modulus. Providing small deformations and considering Bernoulli-Navier hypothesis (during deflection, the plane normal cross-sections of the blade remain plane and normal to the deflected centroidal axis of the blade), the components of the strain vector (arguments x, t are left out) are in the place of the cross-section given by axes η, ζ expressed in the form

$$\varepsilon_x = -\eta \frac{\partial^2 v}{\partial x^2}, \quad \gamma_{xy} = -\zeta \frac{\partial \varphi}{\partial x}, \quad \gamma_{xz} = \eta \frac{\partial \varphi}{\partial x}. \quad (7)$$

In accordance with these assumptions, the potential energy of deformation is written in the form

$$E_p^{(e)} = \frac{1}{2} \int_0^l \int_{(A)} \left[E \left(\eta \frac{\partial^2 v}{\partial x^2} \right)^2 + G \left(\frac{\partial \varphi}{\partial x} \right)^2 (\eta^2 + \zeta^2) \right] dA dx. \quad (8)$$

The transversal deformation of the blade's element is approximated by cubic basis functions

$$\begin{aligned} v(x, t) &= \boldsymbol{\Phi}(x) \mathbf{c}_1(t), & \boldsymbol{\Phi}(x) &= [1 \quad x \quad x^2 \quad x^3], \\ \psi(x, t) &= \frac{\partial v(x, t)}{\partial x} = \frac{\partial \boldsymbol{\Phi}(x)}{\partial x} \mathbf{c}_1 \end{aligned} \quad (9)$$

and the torsional displacement by using linear basis function

$$\varphi(x, t) = \boldsymbol{\psi}(x) \mathbf{c}_2(t), \quad \boldsymbol{\psi}(x) = [1 \quad x]. \quad (10)$$

Let us write the boundary conditions for cases $x = 0$ and $x = l$:

$$\begin{bmatrix} v(0, t) \\ \psi(0, t) \\ v(l, t) \\ \psi(l, t) \end{bmatrix} = \mathbf{q}_1(t) = \underbrace{\begin{bmatrix} 1 & 0 & 0 & 0 \\ 0 & 1 & 0 & 0 \\ 1 & l & l^2 & l^3 \\ 0 & 1 & 2l & 3l^2 \end{bmatrix}}_{\mathbf{S}_1} \mathbf{c}_1(t), \quad \begin{bmatrix} \varphi(0, t) \\ \varphi(l, t) \end{bmatrix} = \mathbf{q}_2(t) = \underbrace{\begin{bmatrix} 1 & 0 \\ 1 & l \end{bmatrix}}_{\mathbf{S}_2} \mathbf{c}_2(t). \quad (11)$$

Now, we can put the vectors of coefficients of the basis functions $\mathbf{c}_1(t)$, $\mathbf{c}_2(t)$

$$\mathbf{c}_1(t) = \mathbf{S}_1^{-1} \mathbf{q}_1(t), \quad \mathbf{c}_2(t) = \mathbf{S}_2^{-1} \mathbf{q}_2(t) \quad (12)$$

into (9), (10) and we get the relations between deformation of the finite blade's element and generalized coordinates of the nodes $i - 1$ and i

$$\begin{aligned} v(x, t) &= \Phi(x) \mathbf{S}_1^{-1} \mathbf{q}_1(t), & \psi(x, t) &= \frac{\partial \Phi(x)}{\partial x} \mathbf{S}_1^{-1} \mathbf{q}_1(t), \\ \varphi(x, t) &= \psi(x) \mathbf{S}_2^{-1} \mathbf{q}_2(t). \end{aligned} \quad (13)$$

During the rotation, due to the centrifugal force, the blade is stretching and the bending resistance is rising. This effect can be described by deformation energy [15]. The extended length of the mass blade's element with original length dx is

$$ds = dx \sqrt{1 + \left(\frac{\partial v}{\partial x} \right)^2}. \quad (14)$$

According to the small deformations, we get from the *Taylor* expansion

$$ds \cong dx \left[1 + \frac{1}{2} \left(\frac{\partial v}{\partial x} \right)^2 \right]. \quad (15)$$

The deformation energy increment in the mass element of the finite blade's element e is caused by work of the centrifugal force $S_0^{(e)}(x)$

$$dE_p^{(e)} = S_0^{(e)}(x) (ds - dx) = \frac{1}{2} S_0^{(e)}(x) \left(\frac{\partial v}{\partial x} \right)^2 dx \quad (16)$$

and in the whole finite blade's element

$$\Delta E_p^{(e)} = \frac{1}{2} \int_0^l S_0^{(e)}(x) \left(\frac{\partial v}{\partial x} \right)^2 dx. \quad (17)$$

If we use the first of the relations (13), the deformation energy increment in the finite blade's element can be in case the constant centrifugal force along the element $S_0^{(e)}(x) = S_0^{(e)}$ rewritten as

$$\Delta E_p^{(e)} = \frac{1}{2} S_0^{(e)} \mathbf{q}_1^T(t) \mathbf{S}_1^{-T} \int_0^l \Phi'^T(x) \Phi'(x) dx \mathbf{S}_1^{-1} \mathbf{q}_1(t). \quad (18)$$

The mathematical model of the undamped finite blade's element is derived by rewriting the *Lagrange's* equations into the mathematical form

$$\begin{aligned} \frac{d}{dt} \left(\frac{\partial E_k^{(e)}}{\partial \dot{\mathbf{q}}^{(e)}} \right) - \frac{\partial E_k^{(e)}}{\partial \mathbf{q}^{(e)}} + \frac{\partial (E_p^{(e)} + \Delta E_p^{(e)})}{\partial \mathbf{q}^{(e)}} = \\ = \mathbf{M}^{(e)} \ddot{\mathbf{q}}^{(e)} + \omega_0 \mathbf{G}^{(e)} \dot{\mathbf{q}}^{(e)} + [\mathbf{K}_s^{(e)} + \omega_0^2 (\mathbf{K}_\omega^{(e)} - \mathbf{K}_d^{(e)})] \mathbf{q}^{(e)}. \end{aligned} \quad (19)$$

Using approximation relations (13) and according to (4), (8), (18) we are able to express the kinetic and potential energy of the blade's element and after simplifications of the identity (19) we get symmetric mass $\mathbf{M}^{(e)}$, static stiffness $\mathbf{K}_s^{(e)}$, bending stiffening $\omega_0^2 \mathbf{K}_\omega^{(e)}$ and softening $-\omega_0^2 \mathbf{K}_d^{(e)}$ matrices and a skew-symmetric matrix of gyroscopic effects $\omega_0 \mathbf{G}^{(e)}$ in the form

$$\begin{aligned} \mathbf{M}^{(e)} &= \rho \begin{bmatrix} A \mathbf{S}_1^{-T} \mathbf{I}_\Phi \mathbf{S}_1^{-1} + J_z \mathbf{S}_1^{-T} \mathbf{I}_{\Phi'} \mathbf{S}_1^{-1} & \mathbf{0} \\ \mathbf{0} & J_p \mathbf{S}_2^{-T} \mathbf{I}_\Psi \mathbf{S}_2^{-1} \end{bmatrix}, \\ \mathbf{G}^{(e)} &= \rho \begin{bmatrix} \mathbf{0} & -J_p \mathbf{S}_1^{-T} \mathbf{I}_{\Phi'} \mathbf{S}_2^{-1} \\ J_p \mathbf{S}_2^{-T} \mathbf{I}_\Psi \mathbf{S}_1^{-1} & \mathbf{0} \end{bmatrix}, \\ \mathbf{K}_s^{(e)} &= \begin{bmatrix} E J_z \mathbf{S}_1^{-T} \mathbf{I}_{\Phi''} \mathbf{S}_1^{-1} & \mathbf{0} \\ \mathbf{0} & G J_k \mathbf{S}_2^{-T} \mathbf{I}_\Psi \mathbf{S}_2^{-1} \end{bmatrix}, \\ \omega_0^2 \mathbf{K}_\omega^{(e)} &= S_0^{(e)} \begin{bmatrix} \mathbf{S}_1^{-T} \mathbf{I}_{\Phi'} \mathbf{S}_1^{-1} & \mathbf{0} \\ \mathbf{0} & \mathbf{0} \end{bmatrix}, \quad \mathbf{K}_d^{(e)} = \begin{bmatrix} \rho J_p \mathbf{S}_1^{-T} \mathbf{I}_\Phi \mathbf{S}_1^{-1} & \mathbf{0} \\ \mathbf{0} & \mathbf{0} \end{bmatrix}. \end{aligned} \quad (20)$$

Each of the blade's elements is defined by quantities A (cross-section area), J_z (the second moment of area of cross-section about the axis z), J_p (the polar second moment of area), J_k (torsion constant) and material parameters ρ (density), E (Young's modulus) and G (shear modulus). In these matrices of the finite blade's element with length l (20), there have been used integral matrices [16]

$$\begin{aligned} \mathbf{I}_\Phi &= \int_0^l \Phi^T(x) \Phi(x) dx, & \mathbf{I}_\Psi &= \int_0^l \Psi^T(x) \Psi(x) dx, \\ \mathbf{I}_{\Phi'} &= \int_0^l \Phi'^T(x) \Phi'(x) dx, & \mathbf{I}_{\Psi'} &= \int_0^l \Psi'^T(x) \Psi'(x) dx, \\ \mathbf{I}_{\Phi''} &= \int_0^l \Phi''^T(x) \Phi''(x) dx, & \mathbf{I}_{\Phi'\Psi} &= \int_0^l \Phi'^T(x) \Psi(x) dx, \end{aligned} \quad (21)$$

where the prime symbol marks derivation with respect to x , the superscript -1 marks inversion and T transposition.

The configuration space defined by (3) is more suitable for the blade's element modeling, because the mass, gyroscopic effects and stiffness matrices have a simple block-diagonal structure. Owing to the blade topology of the chain-type and the sequential numbering of the degrees of freedom, it is useful to transform the blade's element matrices into a configuration space

$$\mathbf{q}_e = [v_{i-1}, \psi_{i-1}, \varphi_{i-1}, v_i, \psi_i, \varphi_i]^T \quad (22)$$

with different displacement arrangement. Then, the global blade's matrices (subscript B) $\mathbf{M}_B, \mathbf{G}_B, \mathbf{K}_{s,B}, \mathbf{K}_{\omega,B}, \mathbf{M}_{d,B}$ have a block-diagonal structure. For this purpose, let us derive a transformational matrix \mathbf{T} :

$$\mathbf{q}^{(e)} = \begin{bmatrix} v_{i-1} \\ \psi_{i-1} \\ v_i \\ \psi_i \\ \varphi_{i-1} \\ \varphi_i \end{bmatrix} = \begin{bmatrix} 1 & 0 & 0 & 0 & 0 & 0 \\ 0 & 1 & 0 & 0 & 0 & 0 \\ 0 & 0 & 0 & 1 & 0 & 0 \\ 0 & 0 & 0 & 0 & 1 & 0 \\ 0 & 0 & 1 & 0 & 0 & 0 \\ 0 & 0 & 0 & 0 & 0 & 1 \end{bmatrix} \begin{bmatrix} v_{i-1} \\ \psi_{i-1} \\ \varphi_{i-1} \\ v_i \\ \psi_i \\ \varphi_i \end{bmatrix} = \mathbf{T} \mathbf{q}_e . \tag{23}$$

Thereafter, the transformed mass $\tilde{\mathbf{M}}^{(e)}$, gyroscopic effects $\omega_0 \tilde{\mathbf{G}}^{(e)}$, static stiffness $\tilde{\mathbf{K}}_s^{(e)}$, bending stiffening $\omega_0^2 \tilde{\mathbf{K}}_\omega^{(e)}$ and softening $-\omega_0^2 \tilde{\mathbf{K}}_d^{(e)}$ matrices of the beam element are expressed in the form

$$\tilde{\mathbf{X}}^{(e)} = \mathbf{T}^T \mathbf{X}^{(e)} \mathbf{T} , \quad \mathbf{X}^{(e)} = \mathbf{M}^{(e)}, \omega_0 \mathbf{G}^{(e)}, \mathbf{K}_s^{(e)}, \omega_0^2 \mathbf{K}_\omega^{(e)}, -\omega_0^2 \mathbf{K}_d^{(e)} . \tag{24}$$

The blade's matrices are comprised of the transformed matrices of all beam elements and they are supplemented with mass, gyroscopic effects and softening under rotation matrices of the rigid blade shroud. After these standard operations and including a material damping of the blade approximated by a proportional damping matrix in the form

$$\mathbf{B}_B = \alpha \mathbf{M}_B + \beta \mathbf{K}_{s,B} , \tag{25}$$

where the coefficients α, β of the proportional damping are calculated from estimated damping ratios of the two lowest bending mode shapes of the blade, the mathematical model of the damped blade with the shroud has the form

$$\mathbf{M}_B \ddot{\mathbf{q}}_B + (\mathbf{B}_B + \omega_0 \mathbf{G}_B) \dot{\mathbf{q}}_B + [\mathbf{K}_{s,B} + \omega_0^2 (\mathbf{K}_{\omega,B} - \mathbf{K}_{d,B})] \mathbf{q}_B = \mathbf{0} , \tag{26}$$

where

$$\mathbf{q}_B = [\dots, v_i, \psi_i, \varphi_i, \dots]^T , \quad i = 1, 2, \dots, N \tag{27}$$

and N is number of nodes, whereas the last node is in the centre of the blade shroud's gravity. In comparison with non-rotating blade ($\omega_0 = 0$), the equations of motion of rotating blade contain a skew-symmetric matrix of gyroscopic effects $\omega_0 \mathbf{G}_B$ and symmetric matrices of bending stiffening under rotation $\omega_0^2 \mathbf{K}_{\omega,B}$ because of the centrifugal forces and softening under rotation $-\omega_0^2 \mathbf{K}_{d,B}$ due to the vibration modeling in rotating space.

3. Model of the couple of blades with friction element

In this work, the friction element is considered a mass point with mass m_e elastically placed in vertical direction in a wedge gap between the blade shrouds and it can do only vertical displacement v_e in the gap.

The mathematical model of the whole system of the couple of blades with the friction element is

$$\begin{aligned}
 & \underbrace{\begin{bmatrix} \mathbf{M}_1 & \mathbf{0} & \mathbf{0} \\ \mathbf{0} & m_e & \mathbf{0} \\ \mathbf{0} & \mathbf{0} & \mathbf{M}_2 \end{bmatrix}}_{\mathbf{M}} \underbrace{\begin{bmatrix} \dot{\mathbf{q}}_1 \\ \ddot{v}_e \\ \dot{\mathbf{q}}_2 \end{bmatrix}}_{\dot{\mathbf{q}}} + \underbrace{\begin{bmatrix} \mathbf{B}_1 + \omega_0 \mathbf{G}_1 & \mathbf{0} & \mathbf{0} \\ \mathbf{0} & 0 & \mathbf{0} \\ \mathbf{0} & \mathbf{0} & \mathbf{B}_2 + \omega_0 \mathbf{G}_2 \end{bmatrix}}_{\mathbf{B} + \omega_0 \mathbf{G}} \underbrace{\begin{bmatrix} \dot{\mathbf{q}}_1 \\ \dot{v}_e \\ \dot{\mathbf{q}}_2 \end{bmatrix}}_{\dot{\mathbf{q}}} + \\
 & + \left(\underbrace{\begin{bmatrix} \mathbf{K}_{s,1} + \omega_0^2 (\mathbf{K}_{\omega,1} - \mathbf{K}_{d,1}) & \mathbf{0} & \mathbf{0} \\ \mathbf{0} & 0 & \mathbf{0} \\ \mathbf{0} & \mathbf{0} & \mathbf{K}_{s,2} + \omega_0^2 (\mathbf{K}_{\omega,2} - \mathbf{K}_{d,2}) \end{bmatrix}}_{\mathbf{K}_s + \omega_0^2 (\mathbf{K}_\omega - \mathbf{K}_d)} + \mathbf{K}_C \right) \underbrace{\begin{bmatrix} \mathbf{q}_1 \\ v_e \\ \mathbf{q}_2 \end{bmatrix}}_{\mathbf{q}} = \quad (28) \\
 & = \underbrace{\begin{bmatrix} \mathbf{f}_1(t) \\ 0 \\ \mathbf{f}_2(t) \end{bmatrix}}_{\mathbf{f}(t)} + \underbrace{\begin{bmatrix} -\mathbf{f}_A(c_A) \\ F_{tA}(c_A) + F_{tB}(c_B) \\ -\mathbf{f}_B(c_B) \end{bmatrix}}_{\mathbf{f}^*},
 \end{aligned}$$

where subscripts 1 and 2 correspond to the blades. The stiffness matrix \mathbf{K}_C of internal elastic couplings between the friction element and the blade shrouds is in its compressed form expressed as

$$\tilde{\mathbf{K}}_C = k_e \begin{bmatrix} 1 & -1 & 0 \\ -1 & 2 & -1 \\ 0 & -1 & 1 \end{bmatrix} \quad (29)$$

and providing discretization of either of the blades on five finite elements, the elements of the compressed stiffness matrix $\tilde{\mathbf{K}}_C$ of internal elastic couplings are in matrix \mathbf{K}_C located on positions of displacements $v_{5,1}$, v_e and $v_{5,2}$ in the generalized coordinate vector $\mathbf{q} = [\mathbf{q}_1^T, v_e, \mathbf{q}_2^T]^T$.

Frictional forces concentrated in central contact points A, B (Figure 2) are approximated by continuous function of corresponding slip velocity

$$c_A = \dot{v}_{5,1} + r_A \dot{\varphi}_{5,1} - \dot{v}_e, \quad c_B = \dot{v}_{5,2} - r_B \dot{\varphi}_{5,2} - \dot{v}_e, \quad (30)$$

where r_A and r_B are perpendicular distances between the contact points and the axes of the blades. The frictional forces respect the new friction characteristic in the form

$$F_{tX} = \begin{cases} N_X [f_d + (f_s - f_d) e^{-d|c_X|}] \text{sign}(c_X), & |c_X| > c_r, \\ N_X \frac{c_X}{c_r} [f_d + (f_s - f_d) e^{-d c_r}], & |c_X| \leq c_r, \end{cases} \quad X = A, B, \quad (31)$$

displayed on Figure 4. The micro- and macro-slip phases are separated by critical slip velocity c_r defining length of the micro-slip velocities interval $-c_r \leq c_X \leq c_r$, $X = A, B$, where the friction is approximated by step line [12]. Normal forces acting in contact areas are determined by friction element geometry and result from the equations of equilibrium in horizontal plane (Figure 5)

$$N_A = m_e r_e \omega_0^2 \frac{\cos(\beta + \delta)}{\sin \beta}, \quad N_B = m_e r_e \omega_0^2 \frac{\cos \delta}{\sin \beta}, \quad (32)$$

where $m_e r_e \omega_0^2$ (in Figure 2 marked as F_C) is centrifugal force acting on the friction element in its centre of gravity.

The vectors of frictional forces in equations of motion (28) can be written in following form :

$$\mathbf{f}_A(c_A) = F_{tA} [0, 0, \dots, 1, 0, r_A]^T, \quad \mathbf{f}_B(c_B) = F_{tB} [0, 0, \dots, 1, 0, r_B]^T. \quad (33)$$

The excitation vectors $\mathbf{f}_j(t)$, $j = 1, 2$ depend on particular realization of the blades' excitation.

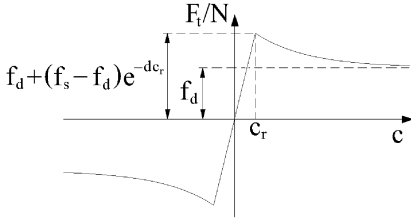


Fig.4: Characteristic of frictional forces in contact areas

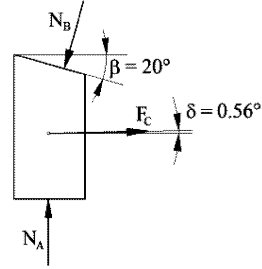


Fig.5: Detail of the friction element placed between the shrouds

For determination of time behaviour of the generalized coordinates, the MATLAB environment is used. First of all the model (28) is rewritten as a system of first-order differential equations in the form

$$\begin{bmatrix} \dot{\mathbf{q}}(t) \\ \ddot{\mathbf{q}}(t) \end{bmatrix} = \begin{bmatrix} \mathbf{0} \\ -\mathbf{M}^{-1} [\mathbf{K}_s + \omega_0^2 (\mathbf{K}_\omega - \mathbf{K}_d) + \mathbf{K}_c] \end{bmatrix} \begin{bmatrix} \mathbf{q}(t) \\ \dot{\mathbf{q}}(t) \end{bmatrix} + \begin{bmatrix} \mathbf{E} \\ -\mathbf{M}^{-1} (\mathbf{B} + \omega_0 \mathbf{G}) \end{bmatrix} \begin{bmatrix} \mathbf{q}(t) \\ \dot{\mathbf{q}}(t) \end{bmatrix} + \begin{bmatrix} \mathbf{0} \\ \mathbf{M}^{-1} [\mathbf{f}(t) + \mathbf{f}^*] \end{bmatrix}, \quad (34)$$

where \mathbf{E} is a unit matrix, and then it is solved with the MATLAB ODE23 numerical solver, which is based on an explicit Runge-Kutta (2,3) pair of Bogacki and Shampine [17].

4. Analysis of the friction characteristic impact on bending vibration of the blade shroud under rotation

Experiments realized in IT AS CR [11] approximately allow to identify parameters f_d (dynamic coefficient of friction), f_s (static coefficient of friction), d (coefficient of decrease) and critical slip velocity c_r separating micro- and macro-slips. In consequence of good conformity of experimentally ascertained transient vibration and numerical simulation results on the model (28) with ARAMID friction element for $\omega_0 = 0$ and after switching off of the electromagnet (jump stopping of the excitation force), we regard the values $f_d = 0.3$, $f_s = 0.6$, $d = 2 \text{ s m}^{-1}$, $c_r = 10^{-3} \text{ m s}^{-1}$ [13] as reference.

Figures 6–9 display transient vibrations of one of the rotating blades (the second one) supposing the harmonic excitation by non-rotating electromagnet producing transversal (in y axis direction) force $F(t) = F_0 \sin 2\pi f_1 t$ with amplitude $F_0 = 15 \text{ N}$ and frequency $f_1 = 131.65 \text{ Hz}$ corresponds to the lowest eigenfrequency of the blade with shroud. The revolution speed of the bladed disk has been chosen as $n = 263.3 \text{ rpm}$, when the excitation under the electromagnet has opposite direction on neighbouring blades. There are compared two different variations of transient vibrations for two values of the coefficient of decrease ($d = 2$, $d = 50$).

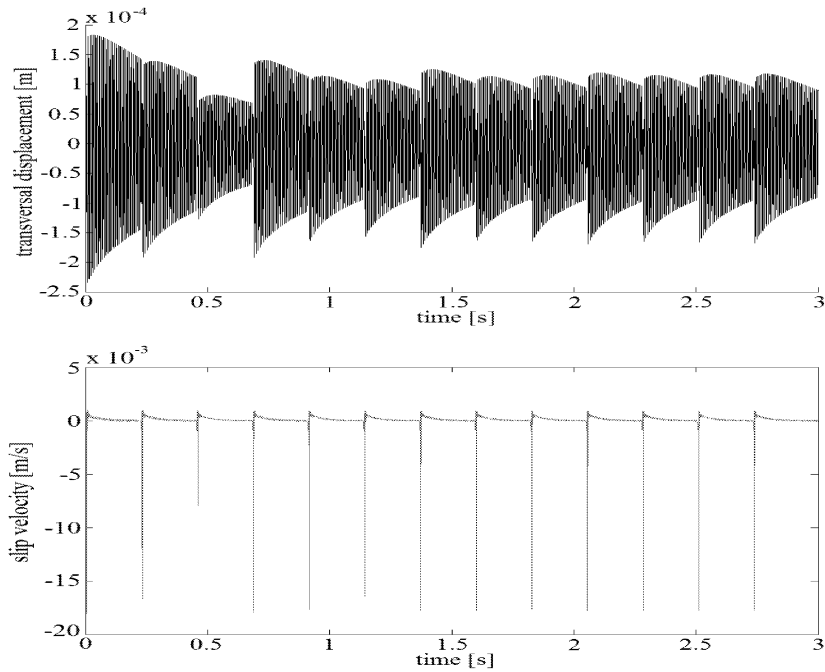


Fig.6: Time behaviour of the blade shroud transversal displacement and slip velocity of this shroud relative to friction element; parameters of the friction characteristic: $f_d = 0.3$, $f_s = 0.6$, $d = 2 \text{ s m}^{-1}$, $c_r = 10^{-3} \text{ m s}^{-1}$

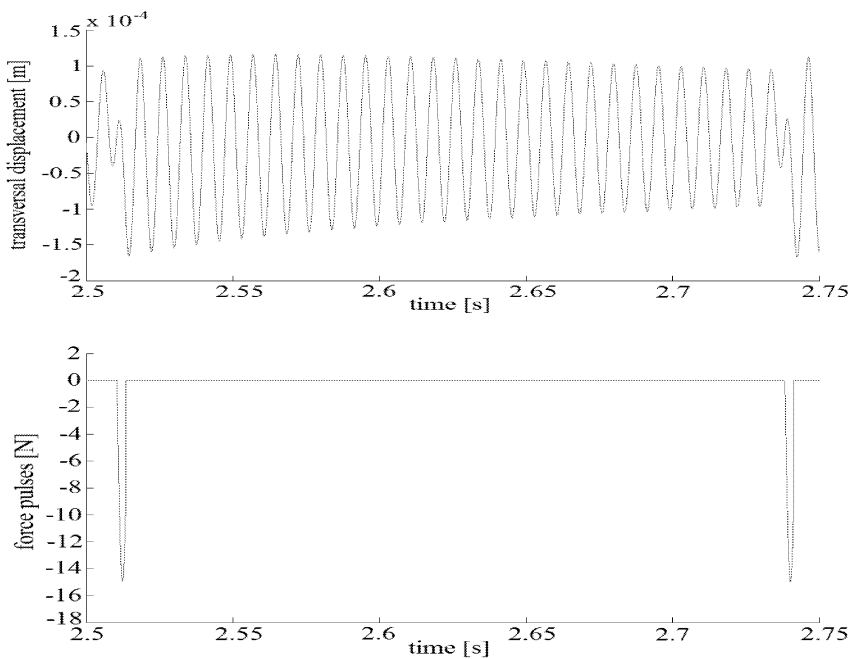


Fig.7: Detail of the blade shroud transversal displacement from Figure 6 and excitation force

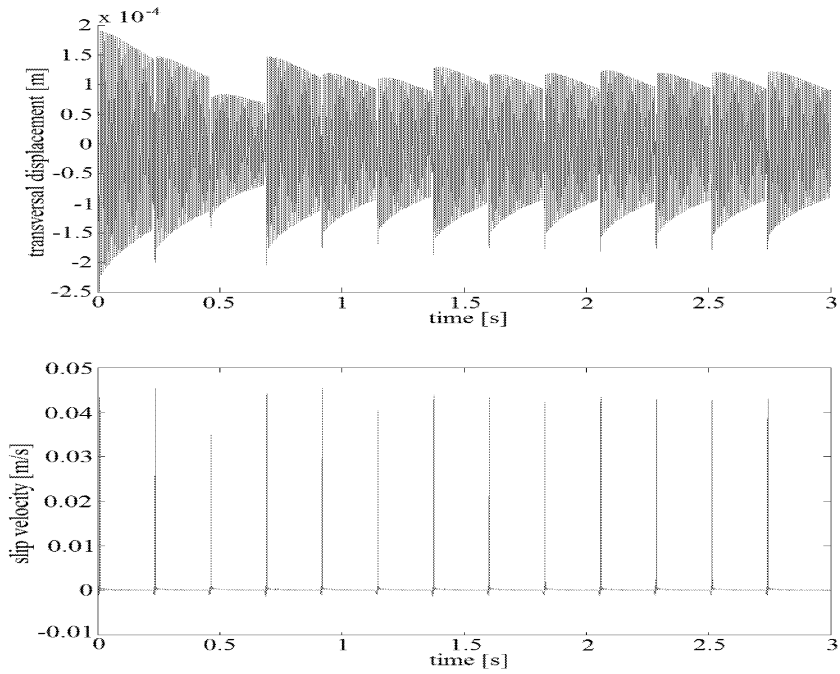


Fig.8: Time behaviour of the blade shroud transversal displacement and slip velocity of this shroud relative to friction element; parameters of the friction characteristic : $f_d = 0.3$, $f_s = 0.6$, $d = 50 \text{ s m}^{-1}$, $c_r = 10^{-3} \text{ m s}^{-1}$

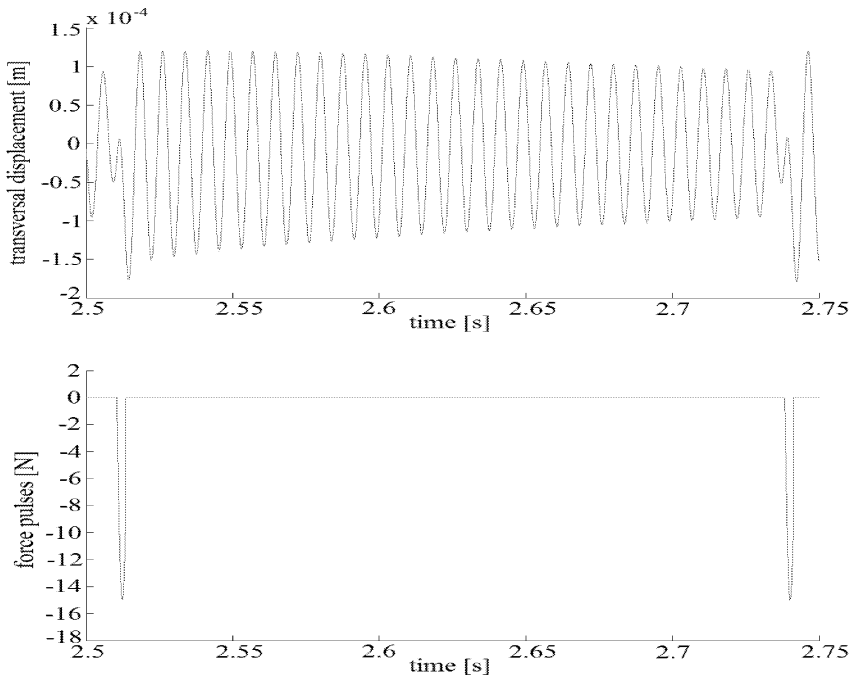


Fig.9: Detail of the blade shroud transversal displacement from Figure 8 and excitation force

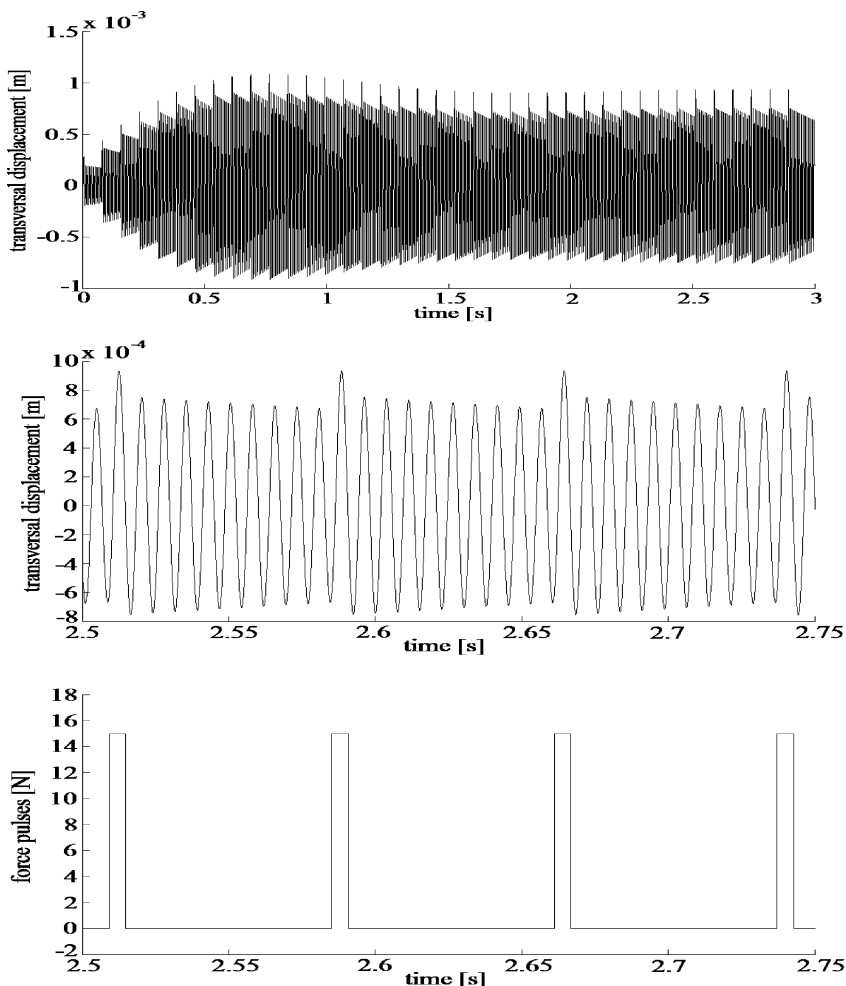


Fig.10: Time behaviour of the blade shroud transversal displacement of model without friction element, detail of this transversal displacement and detail of the resonance force pulse excitation

As the second example of analysis of friction impact in contact areas between the blade shrouds and the friction element, let us suppose transient vibrations of one of the blades (the second one) providing synchronous and resonance excitation realized by two non-rotating electromagnets radially placed (oppositely to each other) in vicinity of the rotating blade shrouds. Excitation of the blades is approximately substituted by rectangular pulses [18] shown on Figures 10–11. The excitation forces acting on blade shrouds are expressed as

$$F_1(t) = F_0 \sum_{k=0}^K \{H(t - k T_b) - H[t - (k T_b + \tau)]\} , \tag{35}$$

$$F_2(t) = F_0 \sum_{k=0}^K \{H[t - (k T_b + \Delta t)] - H[t - (k T_b + \Delta t + \tau)]\} , \tag{36}$$

where $F_0 = 15 \text{ N}$ is amplitude of the rectangular pulses, $T_b = m/f_1$ is period of the resonance pulse excitation, $m = 10$ is ratio of the excitation period to period of the lowest eigenfre-

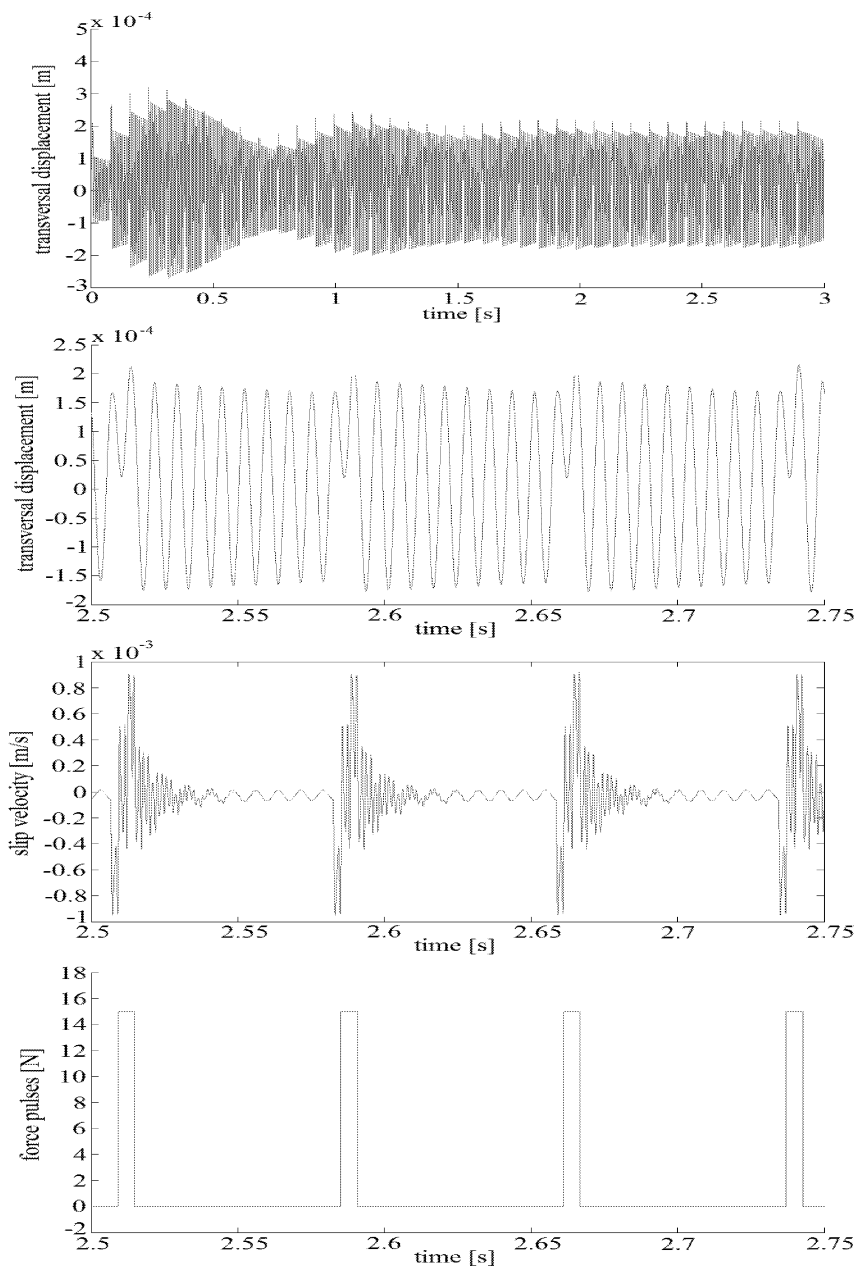


Fig.11: Time behaviour of the blade shroud transversal displacement of model with friction element, detail of this transversal displacement, detail of slip velocity of this shroud relative to friction element and detail of the resonance force pulse excitation

quency of the blade with shroud, $\tau = 0.00566$ s is width of the pulses and $\Delta t = 0.00253$ s is time delay of the pulses on the second blade. Figures 10–11 show the transient vibrations for resonance excitation by revolution speed $n = 394.95$ rpm. Time behaviour of transient vibration of the couple of blades without the friction element ($f_s = f_d = 0$, Figure 10) are compared with time behaviour of transient vibration of the couple of blades with the

friction element and friction characteristic parameters $f_d = 0.3$, $f_s = 0.6$, $d = 2 \text{ s m}^{-1}$, $c_r = 10^{-3} \text{ m s}^{-1}$ (Figure 11).

5. Conclusions

Designed computational model of the rotating couple of blades with friction element allows to analyse impacts of the parameters of characteristic of frictional forces, acting in central contact points between the blade shrouds and the friction element, and angular velocity of the bladed disk on bending and torsional blade vibrations. This paper deals with two different analyses of friction impact on bending blade vibration providing steady bladed disk's rotation with constant angular velocity ω_0 . For this reason, the model of the blades has been supplemented with matrices of gyroscopic effects, bending stiffening under rotation because of the centrifugal forces and softening under rotation due to the vibration modeling in rotating space. Connecting of the friction element to the blade shrouds has been realized by using springs situated transversely to the blades' axes.

In the first task, excitation of the blades has been performed by one non-rotating electromagnet placed in vicinity of the rotating blade shrouds. Evoked magnetic field has acted on blade shrouds by harmonic varying force with the frequency corresponding to the lowest eigenfrequency of the blade with shroud. The revolution speed of the bladed disk has been chosen to ensure the opposite direction of the excitation on neighbouring blades. In comparison with the variant $d = 50$, lower value of the coefficient of decrease of the friction characteristic ($d = 2$) has entailed considerably lower slip speeds of the blade shrouds relative to the friction element and partially also bending vibration suppression of the blades.

The second task has been focused on investigation of importance of the friction element embedded into a wedge gap between the blade shrouds in case synchronous and resonance transversal excitation realized by two non-rotating electromagnets radially placed (oppositely to each other) in vicinity of the rotating blade shrouds. Owing to dissipation of energy in contact areas, inserting of the friction element into the gap has a positive effect in decreasing of extreme values of transversal amplitudes of the blade shrouds by 30 %.

Acknowledgement

This work has been elaborated in a frame of the grant project GA CR 101/09/1166 'Research of dynamic behaviour and optimization of complex rotating system with non-linear couplings and high damping materials'.

References

- [1] Cigeroglu E., An N., Meng C.H.: A microslip friction model with normal load variation induced by normal motion, *Nonlinear Dynamics*, 50 (2007) 609–626
- [2] Firrone C.M., Zucca S.: Underplatform dampers for turbine blades: The effect of damper static balance on the blade dynamics, *Mechanics Research Communications*, 36 (2009) 515–522
- [3] Borrajo J.M., Zucca S., Gola M.M.: Analytical formulation of the Jacobian matrix for non-linear calculation of forced response of turbine blade assemblies with wedge friction dampers, *International Journal of Non-linear Mechanics*, 41 (2006) 1118–1127
- [4] Csaba G.: Forced response analysis in time and frequency domains of a tuned bladed disk with friction dampers, *Journal of Sound and Vibrations*, 214 (1998) 395–412
- [5] Brepta R., Půst L., Turek F.: *Mechanical vibration*, Sobotáles, Praha, 1994 (in Czech)
- [6] Sextro W.: *Dynamical Contact Problems with Friction*, Springer, Berlin, Heidelberg, 2007

- [7] Zeman V., Byrtus M., Hajžman M.: Harmonic forced vibration of two rotating blades with friction damping, *Engineering Mechanics*, 17 (2010) 187
- [8] Půst L., Pešek L., Veselý J., Radolfová A.: Detuning impact of a beam with frictional damper on resonance tops heights, Research report Z-1441/09, IT AS CR, v.v.i, 2009 (in Czech)
- [9] Půst L., Horáček J., Radolfová A.: Vibrations of beams with frictional surfaces on perpendicular shrouds, Research report Z-1421/08, IT AS CR, 2008 (in Czech)
- [10] Brůha J., Zeman V.: Detuning Impact of Couple of Blades with Friction Element on Bending Vibration, *Engineering Mechanics*, 18 (2011) 237
- [11] Pešek L.: Vibration Attenuation of the Blade Couple Damped by ARAMID Friction Element, Extract from research report, IT AS CR
- [12] Půst L., Pešek L., Radolfová A.: Various Types of Dry Friction Characteristics for Vibration Damping, *Engineering Mechanics*, 18 (2011) 203
- [13] Brůha J., Zeman V.: Friction Characteristic Impact on Bending Vibration of Couple of Blades with Friction Element, In: Extended abstracts of Computational Mechanics 2011, University of West Bohemia in Pilsen, 2011
- [14] Slavík J., Stejskal V., Zeman V.: Basics of machine dynamics, ČVUT, Praha, 1997 (in Czech)
- [15] Géradin M., Rixen D.: Mechanical vibration, John Wiley and Sons, Chichester, 1997
- [16] Byrtus M., Hajžman M., Zeman V.: Dynamics of Rotating Systems, University of West Bohemia in Pilsen, 2010 (in Czech)
- [17] Příklad P., Brandner M.: Numerical methods II, ZČU, Plzeň, 2000 (in Czech)
- [18] Pešek L., Vaněk F., Bula V., Cibulka J.: Excitation of Blade Vibration under Rotation by Synchronous Electromagnet, *Engineering Mechanics*, 18 (2011) 249

Received in editor's office: April 15, 2012

Approved for publishing: September 18, 2012